Pergamon

Tetrahedron 58 (2002) 197–204

TETRAHEDRON

Studies of stereoselectivity in cycloaddition of cyclic dienes to 2-azabicyclo[2.2.2]octene derivatives; through-space effects on ^{15}N NMR shifts of bicyclic amines and lactams

John R. Malpass,[a,*] Djaballah Belkacemi[b] and David R. Russell[a]

[a]*Department of Chemistry, University of Leicester, Leicester LE1 7RH, UK*
[b]*Département de Chimie, Institut des Sciences Exactes, Centre Universitaire Oum El Bouaghi, Oum El Bouaghi, 040000, Algeria*

Received 2 October 2001; accepted 15 November 2001

Abstract—Only two of the four possible facial approaches of cyclohexa-1,3-diene to the double bond in 2-methyl-5,6-benzo-2-azabicyclo[2.2.2]oct-7-en-3-one 7 are observed, giving *exo*,*endo*- and *endo*,*endo*-Diels–Alder cycloadducts **10a** and **11a** at atmospheric pressure (*exo*- and *endo*-defined here by reference to the benzo- and etheno-bridges, respectively). Hydride reduction of the carbonyl in **10a** provides an indirect route to **9**, which is formally derived from 2-methyl-5,6-benzo-2-azabicyclo[2.2.2]oct-7-ene **6** but which is inaccessible directly owing to thermal retro-cycloaddition of **6**. X-Ray crystal structures confirm the stereochemical assignments. Cycloaddition of cyclopentadiene to **7** follows a similar path and the results are compared with corresponding studies on 7-azabicyclo[2.2.1]-heptene analogues where only *exo*-facial attack is observed. Through-space interactions with proximate etheno- and ethano-bridges give rise to substantial upfield ^{15}N NMR shifts of amino and lactam nitrogen.

1. Introduction

The Diels–Alder cycloaddition of 4π components to unsaturated bicyclic alkenes and hetero-bridged analogues has been widely investigated.[1] Continuing developments in the construction of molecular arrays based on norbornyl and heteronorbornyl skeleta have prompted renewed interest in the understanding and control of facial selectivity in the reactions of more complex bicyclic alkenes but most of the work has involved bicyclo-[2.2.1]heptene (norbornenyl) and hetero-norbornenyl derivatives.[1,2] *exo*-Facial selectivity with respect to the norbornenyl partner is generally observed in both carbon- and hetero-bridged systems[1] but two possible approaches are still possible for the diene itself, leading to adducts in which the second ring junction is *exo*-**4** or *endo*-**5** with respect to the second bicyclic unit (Scheme 1). Cycloaddition of reactive isoindoles to 7-oxabenzo-norbornadienes[3] (1,4-dihydro-1,4-epoxynaphthalenes) **1** and *N*-alkoxycarbonyl benzazanorbornadienes[4] **2** gave mixtures of *exo*,*exo* and *exo*,*endo*-cycloadducts (Scheme 1). More recently, Warrener has investigated *exo*,*exo* and *exo*,*endo*-facial selectivity in addition of furans and pyrroles to **1** and **2**[1] but cycloadditions involving pyrrole derivatives required high pressure (14 kbar). Our own studies have extended the range of hetero-norbornene derivatives

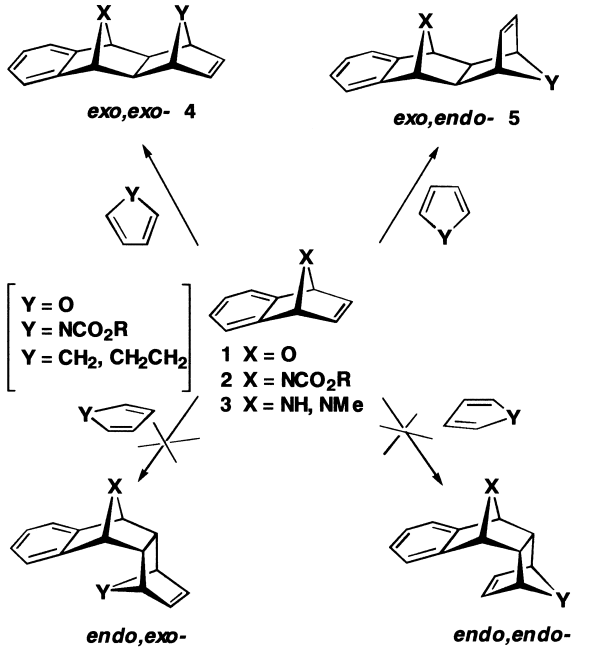

Scheme 1.

accessible at atmospheric pressure to include the first amines **3** (X=NH, NMe) and have also widened the range of 4π components to include cyclic dienes;[5,6] of the four possible stereoisomers, only *exo*,*endo*-adducts **5** (X=NH, NMe, Y=CH_2, CH_2–CH_2) were observed.

Keywords: cycloaddition; stereoselection; bicyclic heterocyclic compounds; NMR.

* Corresponding author. Tel.: +44-116-252-3789; fax: +44-116-252-2126; e-mail: jrm@le.ac.uk

0040–4020/02/$ - see front matter
PII: S0040-4020(01)01125-5

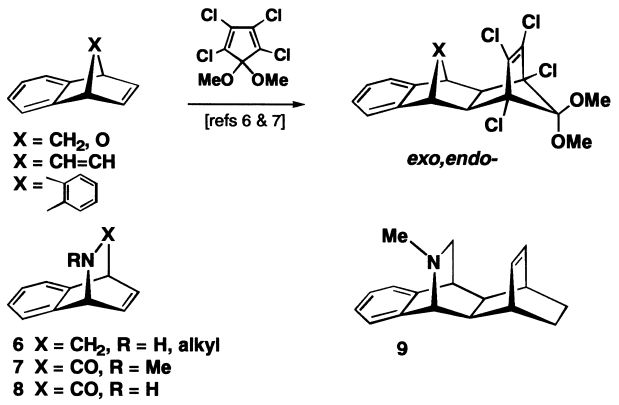

Scheme 2.

nation of structure of the adducts, and selected further transformations.

2. Results

The lactam **7** was heated with 3 molar equiv. of neat cyclohexa-1,3-diene in a sealed tube at 180°C for 16 h. The ^{1}H NMR spectrum revealed the presence of two of the four possible 1:1 adducts (Scheme 3) in a ratio of 78:22. The sense of facial attack on **7** is defined here by reference to the benzo-group in order to maintain consistency with the descriptions of the norbornene-based systems in Scheme 1.[9]

The two compounds had similar R_f values but were separated by fractional crystallisation. The conclusion that one

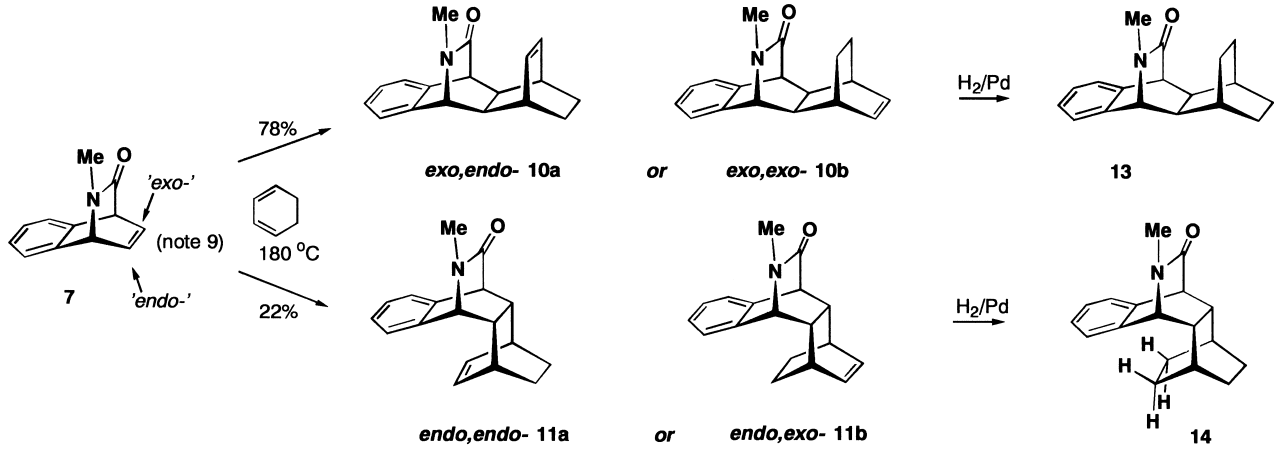

Scheme 3.

We now report extension of these studies to include 2-azabicyclo[2.2.2]octene derivatives in which the nitrogen atom is no longer symmetrically placed with respect to the incoming diene.

The addition of dienes to all-carbon bicyclo[2.2.2]octene (benzobarrelene) derivatives is illustrated by the work of Paquette and Dunkin using 1,2,3,4-tetrachloro-5,5-dimethoxycyclopentadiene which give single cycloadducts (Scheme 2).[7] Williams[8] has applied ab initio methods to the Diels–Alder cycloaddition between bicyclo[2.2.2]octa-2,5-diene-2,3-carboxylic acid and cyclopentadiene and finds a distinct preference for attack from the *endo*-face. We are aware of no experimental studies on azabicyclo[2.2.2]-octene derivatives. Direct addition of cyclic dienes to amines such as **6** is unfortunately not possible owing to competitive thermal retro-cycloaddition to give naphthalene. However, as part of our investigations into possible effects on ^{15}N chemical shifts of through-space interactions between amino-nitrogen and π-bonds,[6] we wished to prepare the system **9** in which the nitrogen is unsymmetrically placed with respect to the π-bond.

The use of the bicyclic lactam **7** was intended to allow primary cycloaddition followed by later removal of the carbonyl group using hydride reduction. We now describe the successful cycloaddition of cyclic dienes to **7**, determi-

cycloadduct resulted from attack from the *exo*-face of **7** and one from the *endo*-face followed from the results of catalytic hydrogenation experiments which gave two *different* products **13** and **14** from samples of the two separate cycloadducts. Clearly, if both adducts had resulted from *exo*-attack on **7** (giving compounds **10a** and **10b**) or, alternatively, if both had resulted from *endo*-attack (giving compounds **11a** and **11b**), a single hydrogenation product would have been formed. The ^{1}H NMR spectrum of **14** showed signals at δ 0.4 (1H), 0.6 (1H), and 0.8 (2H) which were assigned to the ethano-bridge protons, substantially shielded by the ring current of the benzo-group. These

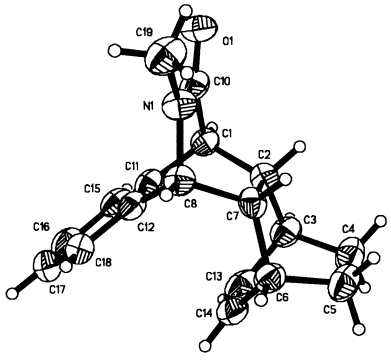

Figure 1. Crystal structure of **11a**.

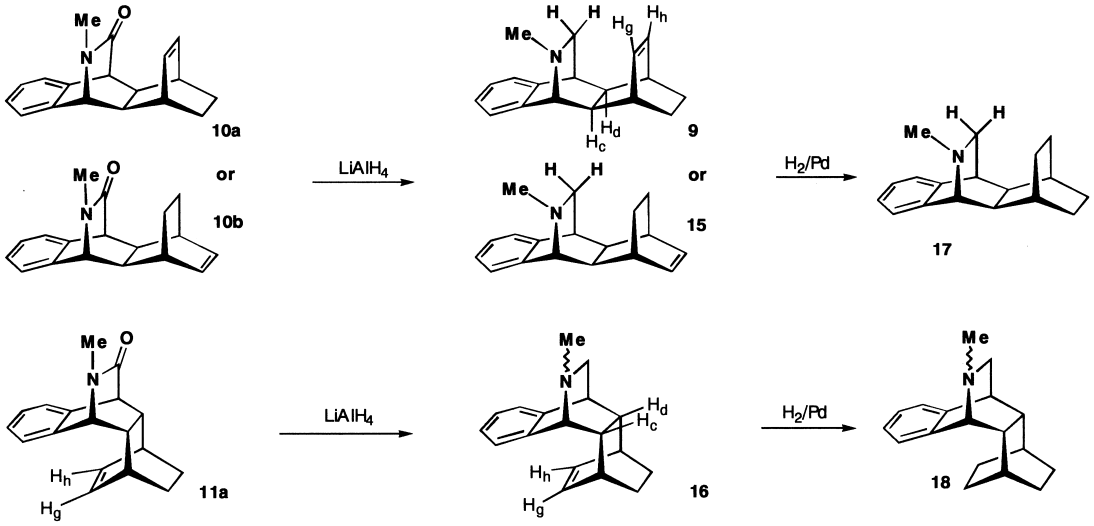

Scheme 4.

characteristic signals were not seen in any of the primary cycloadducts, ruling out **11b** as a possible structure and identifying **11a** as the minor stereoisomer, the product of *endo*-attack on **7**.The *endo*,*endo* stereostructure for **11a** was ultimately confirmed by an X-ray crystal structure (Fig. 1). Unfortunately, data on the major isomer **10a/b** could not be fully refined.

Reduction of the lactam **10a/b** using $LiAlH_4$ gave the amine **9/15** (Scheme 4); similar reduction of **11a** gave **16**.

Table 1. ^{1}H NMR data for lactam cycloadducts and derived amines

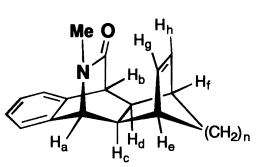
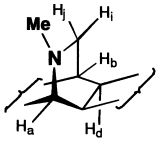
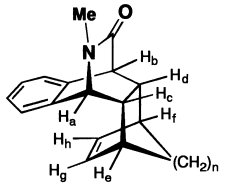
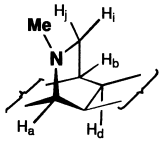

	19 (*n*=1)	**10a** (*n*=2)	**9** (*n*=2)	**20** (*n*=1)	**11a** (*n*=2)	**16** (*n*=2)
H_a	4.25 d	4.23 d	3.36 d	4.23 d	4.17 d	3.39 d
H_b	3.58 d	3.57 d	2.63 ddd	3.69 d	3.62 d	2.75 ddd
H_c	2.43 ddd	1.96 ddd	1.75 ddd	3.08 ddd	2.58 ddd	2.57 ddd
H_d	2.49 ddd	2.03 ddd	1.55 dddd	2.86 ddd	2.42 ddd	2.19 ddd
H_e	2.86 m	2.67 ddd	2.56 bd	2.61 bs	2.36 m	2.2 bd
H_f	2.86 m	2.75 ddd	2.43 bd	2.68 bs	2.36 m	2.3 bd
H_g	6.05 dd	6.17 m	6.2 bdd	4.74 dd	4.88 bdd	4.95 ddd
H_h	6.12 dd	6.17 m	6.15 bdd	4.86 dd	5.00 bdd	5.03 ddd
H_i		3.1 dd				3.3 dd
H_j		1.47 ddd				1.76 dd
$(CH_2)_n$	1.45 bd/1.64 bd(2H)	1.2–1.5 (4H)	1.2–1.4 (4H)	1.45 bd/1.38 bd (2H)	1.05–1.45 bm (4H)	1.1 bd/1.5 bd (4H)
Nme	2.74 s	2.81 s	1.94 s	2.92 s	2.92 s	2.03 s
Benzo-	7.13 m	7.15 m	7.0–7.2 m	6.9–7.2 m	6.9–7.2 m	6.9–7.2 m
$J_{a,c}$	1.9	1.7	2.5	3.5	3.1	3.1
$J_{b,d}$	2.2	2.1	2.0	2.7	2.3	2.0
$J_{c,d}$	9.7	9.9	11.0	9.8	9.8	10.0
$J_{c,g}$ $J_{d,h}$			<1 Hz			
$J_{d,f}$	3.4	2.5	2.0	3.6	1.71.7	2.3
$J_{c,e}$	3.2	1.7	1.8	3.5	2.0	2.0
$J_{f,h}$	3.0	4.5	6.0	3.0	6.0	5.6
J_{e,CH_2}	1.8			1.8		
J_{f,CH_2}	1.8			1.8		
$J_{f,g}$		1.7	<2			1.5
$J_{e,g}$	3.0	4.5	6.0	3.0	6.0	5.6
$J_{e,h}$			<2		1.7	1.5
$J_{g,h}$	5.7	8.0	8.0	5.6	8.1	8.1
J_{gem} (CH_2)	8.1			8.1		
$J_{i,j}$			10.0			9.8
$J_{b,i}$			2.3			2.1
$J_{b,j}$			2.0			2.6
$J_{d,j}$			1.5			

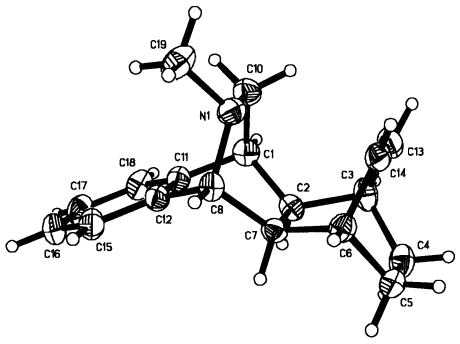

Figure 2. Crystal structure of **9**.

Small-scale hydrogenation of these amines gave two saturated amines **17** and **18** which were shown to be different by ^{1}H NMR spectroscopy, further supporting the proposed *exo*- and *endo*-cycloaddition pathways.

Examination of selected ^{1}H NMR shifts for the adducts (Table 1) showed an *N*-methyl signal for **11a** at δ 2.92 and similar shifts were observed for 13 and 14 δ 2.94 and 2.92, respectively). The upfield shift δ 2.81) for **10a/b** is indicative of an additional anisotropic effect; this is possible only in the case of **10a** which has a nearby etheno-bridge.

The substantial relative upfield shifts shown by the alkene protons H_g and H_h (Scheme 4) in the lactam **11a** and the amine **16** confirm the anisotropic effect of the benzo-ring on the protons of the etheno-bridge. The *endo*,*endo*-geometry in **16** means that there is no restriction on inversion at the amino-nitrogen and the chemical shift of δ 2.03 is reasonable for such an *N*-methyl group.[11,12] In contrast, the invertomer population in either **9** or **15** will be heavily weighted towards the invertomer having the *syn*-*N*-methyl configuration[11] and the relative upfield shift (δ 1.94) is again the result of the anisotropic effect of the benzene ring. This observation does not distinguish absolutely between **9** and **15** but additional evidence was provided by sharpening of the signals due to H_g on selective irradiation of H_c (and corresponding sharpening of H_h on irradiation of H_d); these small 'w'-couplings $J_{c,g}$ and $J_{d,h}$ are consistent with **9** but not **15**. The assignment of **9** (and hence **10a**) was later confirmed beyond any doubt by an X-ray structure (Fig. 2) which also places the *N*-methyl group *syn*- to the benzene ring. The corresponding cycloaddition reactions of **7** with cyclopentadiene followed the same path (Scheme 5) giving **19/20** in a ratio of 65:35.

Stereostructures were confirmed by direct comparison with the higher homologues **10a** and **11a**. Table 1 shows a full assignment of the spectra for all four adducts.

3. Discussion

3.1. Stereoselection

The move from 7-azabicyclo[2.2.1]heptene to 2-azabicyclo[2.2.2]octene derivatives clearly removes the exclusive *exo*-facial attack in both examples although a preference for attack *syn*- to the lactam bridge (*anti*- to the benzo-ring) remains with both dienes. This is in accord with calculations (AM1 and 3-21G and 6-31G*//3-21G methods) carried out on the secondary lactam **8** which predict much smaller energy differences between addition of cyclopentadiene (and cyclohexadiene) to the two faces of the double bond in **8** when compared with the amine **3** (X=NH).[10] In addition, calculations of the energy of all possible products show that the most stable products are not observed, confirming the operation of kinetic, rather than thermodynamic, control in these reactions. At the highest level employed (MP2/6-31G*//3-21G), the difference in calculated transition state energies was even smaller, suggesting that there is no large difference between the two different approaches of cyclopentadiene to the dienophile.[10] Strong repulsive interactions were identified between the methylene proton and the lactam bridge in the transition state leading to **21** and between the methylene proton and the benzo-ring in the transition state leading to **22** (Scheme 5); these were considered to be the cause of the higher activation energies in these cases.

A similar picture emerged from the calculations on the corresponding reaction with cyclohexadiene.[10] Here, strong destabilising interactions were identified between the nitrogen lone pair and a methylene group of the ethano-bridge in the transition state leading to **10b** (Scheme 3) and between the corresponding methylene protons and the benzene π-cloud in the transition state leading to **11b**, rationalising the absence of these two products experimentally.

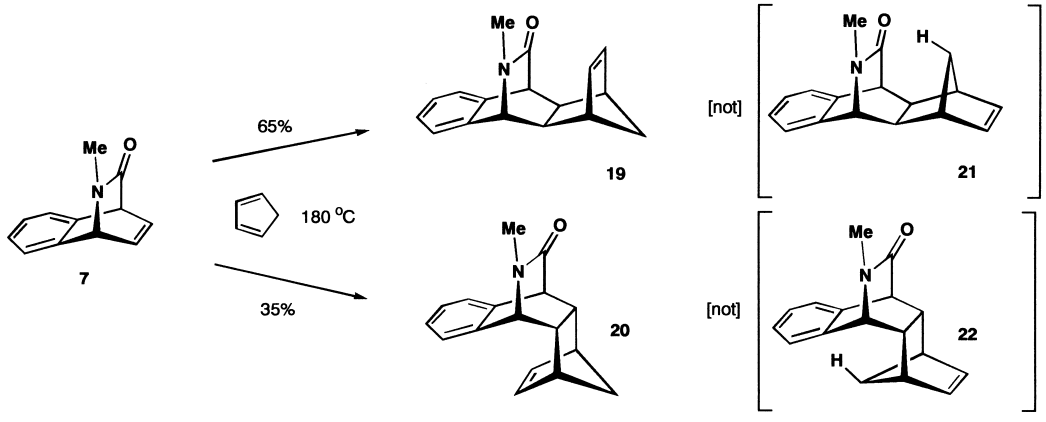

Scheme 5.

Having established the facial selectivity in attack on the double bond, the stereoselectivity resulting from the two possible approaches of the diene to each face requires discussion. The experimental results are clear: the diene approaches so as to place the new etheno-bridge on the same face as the lactam bridge in **10a** and **19** and on the same face as the benzo-group in **11a** and **20**. The AM1 method (again using the secondary amide **8** rather than **7**) fails to predict this result[10] but ab initio studies correctly predicted the formation of **19** and **20** from cyclopentadiene with a modest preference for **19**, as observed experimentally.

In summary, the agreement with the calculations is good and the comparison with earlier additions to 7-azabenzonorbornadiene systems confirm that the *exo*-selectivity with respect to the bicyclo[2.2.1]heptene system is lost on moving to the bicyclo[2.2.2]octene homologues. The approach of the diene to either face of the π-bond in **7** demonstrates total stereoselection producing only the *endo*-ring junction with respect to the new bicyclo[2.2.1]-heptene or bicyclo[2.2.2]octene fragment.

3.2. Proximity effects on ^{15}N NMR shifts

The sensitivity of ^{15}N NMR shifts to ring size and environment is well established and we have shown earlier that upfield shifts result from placement of an etheno-bridge adjacent to the amino-nitrogen in derivatives of the 7-azabicyclo[2.2.1]heptane system.[6]

Examples are shown in Fig. 3. Thus, a relative upfield shift of 12.4 ppm is observed on moving from *syn*-**23**→**24**; the corresponding shift difference for *syn*-**23**→**26** is 13.7 ppm. The comparison is made with *syn*-**23** since the cycloadducts are all present as a single invertomer having the methyl substituent *syn*- to the aryl ring.

A further small *downfield* shift is seen on saturation of the etheno-bridge in **25** and **27**; the placement of the nitrogen between the two CH bonds of the ethano-bridge presumably presents a smaller overall interaction with nitrogen than the π-bond in **24** or **26**. Moving to the novel 2-azabicyclo[2.2.2]octane-based amines, all of the shifts are approximately 60 ppm upfield of the lower homologues, illustrating very clearly the removal of the 'bicyclic' effect (which leads consistently to unusually low-field signals only in 7-azabicyclo[2.2.1]heptanes[5,6,13]). The effect of the fluorine substituents in the aryl ring in **23**–**27** has been shown to have a minimal effect (<2 ppm) and this is neglected here.

The cycloadduct **9** provides an opportunity to see the effect of overlap of the amine lone pair with the terminus of the neighbouring etheno-bridge (rather than the centre of the bond as in **24** and **26**); a similar upfield shift (9.1 ppm) is seen here, relative to the unhindered isomer **16**.

The lactams **10a** and **19** complete a consistent picture, showing upfield shifts (6.2 and 7.3 ppm, respectively) by comparison with the unhindered reference molecules **11a** and **20**. The interaction here is between the p-orbital of the alkene π-system and a p-orbital of the planar delocalised amide group, rather than with the sp^3-hybridised lone pair in the amines, but the effect is qualitatively similar. The ethano-bridged system **13** presents an interesting final comparison since there is a further upfield shift of 9.1 ppm on hydrogenation. This substantial additional increment indicates that the nitrogen p-orbital is now suffering a more serious interaction at the terminus of the π-bond than did the sp^3 amino-nitrogen lone pair with the centre of the π-bond in **25** and **27**. These data add to the developing picture of the sensitivity of nitrogen chemical shifts to the effects of groups which are nearby in space[14] and that such proximity effects lead consistently to upfield shifts.

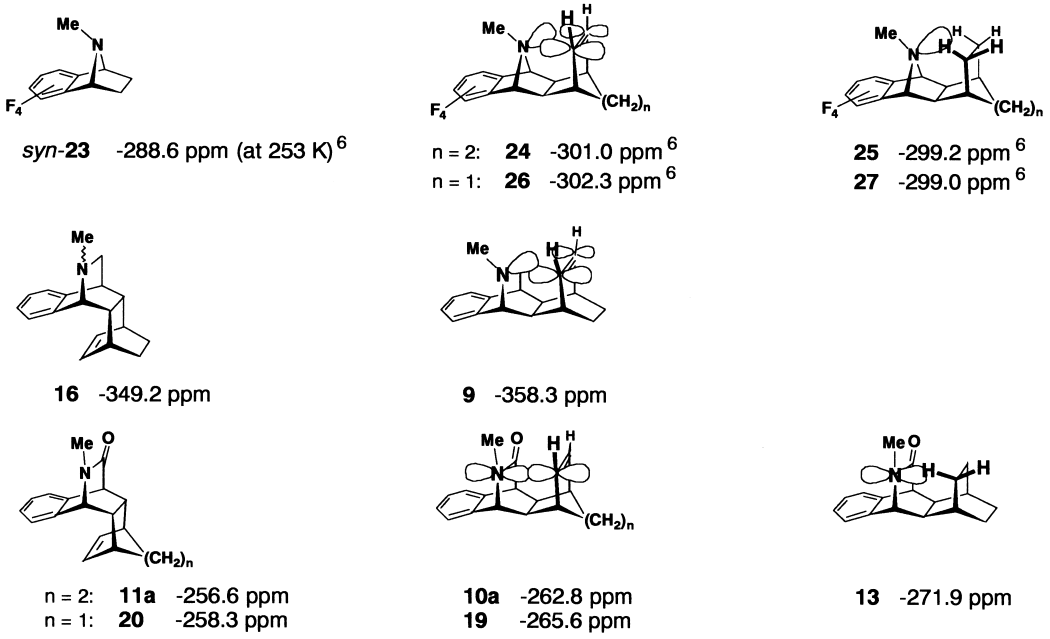

Figure 3. ^{15}N NMR shifts for selected amines and lactams (shifts upfield from nitromethane).

4. Experimental

4.1. General

NMR spectra were recorded on Bruker AM 300, and DRX 400 spectrometers in $CDCl_3$ solvent with TMS as internal reference; ^{13}C assignments were based on DEPT spectra. ^{15}N NMR spectra were recorded at natural abundance in $CDCl_3$ in 10 mm tubes and referenced to neat CH_3NO_2 in an internal 5 mm coaxial tube. IR spectra were recorded on a Perkin–Elmer 298 spectrometer as solutions (CH_2Cl_2). Mass spectra were measured routinely on VG Micromass 16B (EI) or Micromass Quattro LC (ES) spectrometers (base peak shown thus: *). Accurate mass measurements were obtained using a Kratos Concept mass spectrometer (FAB). Silica Gel 60 (Fischer) was used for column and chromatotron separations. TLC was conducted on standard commercial aluminium sheets pre-coated with a 0.2 mm layer of silica gel.

4.1.1. Reaction of 2-methyl-5,6-benzo-2-azabicyclo-[2.2.2]oct-7-ene-3-one 7 with cyclohexa-1,3-diene. To lactam **7**[15] (2.0 g; 10.8 mmol) was added neat cyclohexa-1,3-diene (2.04 ml; 21.0 mmol)) in a Young's tube which was heated overnight (16 h) at 175°C. After cooling, the reaction mixture was placed on a silica column and the excess cyclopentadiene was washed off with petrol (bp 40–60°C). The column was then washed with diethyl ether to elute the reaction products. The ^1H NMR spectrum showed the presence of two cycloadducts **10a** and **11a** in a ratio of 78:22 but the compounds could not be separated chromatographically. Fractional crystallisation using propanone/diethyl ether (80:20) provided samples of each isomer. The adduct **10a** (0.95 g; 33%) was isolated as colourless crystals, mp 210–212°C; ^1H NMR data ($CDCl_3$) are summarised in Table 1; ^{13}C NMR ($CDCl_3$,75 MHz) δ 25.6, 26.1 (CH_2), 32.6 (CH_3), 33.8, 34.2, 44.0, 44.7, 52.8, 64.3, 121.3, 124.0, 126.0, 127.3, 129.7, 130.7 (CH), 140.0, 141.2 (C), 171.9 (CO); ν_{max} (CH_2Cl_2) 3020w, 2940m, 2850w, 1665s, 1455m, 1400m, 1160w, 1030w, 1000w; MS *m/z* 265 (M^+), 159, 127, 51, 42, 32, 28*; Analysis calcd for $C_{18}H_{19}NO$ C 81.47, H 7.22, N 5.28; found: C 81.23, H 7.12, N 5.45%.

The isomer **11a** (0.27 g; 10%) was isolated as colourless crystals, mp 147–149°C; ^1H NMR data ($CDCl_3$) are summarised in Table 1; ^{13}C NMR ($CDCl_3$, 75 MHz) δ 25.7, 26.0 (CH_2), 32.0 (CH), 31.25 (CH_3), 33.5, 40.6, 45.4, 52.6, 63.7, 122.1, 124.6, 126.1, 126.9, 127.4, 127.5 (CH), 136.7, 138.1 (C), 173.7 (CO); ν_{max} (CH_2Cl_2) 3020w, 2940m, 2850w, 1665s, 1455m, 1400m, 1160w, 1030w, 1000w; MS *m/z* 265 (M^+), 159, 127, 51, 42, 32, 28*; Analysis calcd for $C_{18}H_{19}NO$ C 81.47, H 7.22, N 5.28; found: C 81.27, H 7.14, N 5.27%.

4.1.2. Hydrogenation of 10a. A sample of lactam **10a** (0.182 g; 0.68 mmol) was dissolved in methanol (30 ml) and hydrogenated over 5% palladium on carbon at atmospheric pressure for 6 h. The catalyst was filtered off through celite and the solvent removed under reduced pressure. Recrystallisation from propanone: diethyl ether (80:20) gave colourless crystals of **13** (0.166 g; 91%), mp 195–197°C; ^1H NMR ($CDCl_3$, 300 MHz) δ 1.35–1.48 (m, 4H), 1.55–1.62 (m, 4H), 1.83 (s, 4H), 2.94 (s, 3H), 3.74 (brs, 1H), 4.30 (brs, 1H), 7.18 (m, 4H); ^{13}C NMR ($CDCl_3$, 75 MHz) δ 20.9, 22.0, 28.2, 28.5 (CH_2), 33.2 (CH_3), 28.7, 28.8, 40.2, 42.4, 52.7, 64.5, 121.2, 124.2, 126.1, 127.2 (CH), 139.9, 141.6 (C), 174.3 (CO); ν_{max} (CH_2Cl_2) 3030w, 2940s, 2910s, 2865m, 1665s, 1485m, 1460m, 1400m, 1230m, 1180w, 1050w; M.S. *m/z* 267 (M+), 159*, 32, 28; Analysis calcd for $C_{18}H_{21}NO$ C 80.86, H 7.91, N 5.23; found: C 80.67, H 7.78, N 5.40%.

4.1.3. Hydrogenation of 11a. A sample of lactam **11a** (0.035 g; 0.132 mmol) containing a trace of **10a** was hydrogenated as described for **10a** to give crystals of **14** contaminated with a trace of **13**; ^1H NMR ($CDCl_3$, 300 MHz) δ 0.40 (m, 1H), 0.60 (m, 1H), 0.80 (m, 2H), 1.50 (m, 5H), 1.65 (m, 1H), 2.30 (brd, 1H, J=11.5 Hz), 2.45 (brd, 1H, J=11.5 Hz) 2.92 (s, 3H), 3.80 (d, 1H, J=2.4 Hz), 4.33 (d, 1H, J=3.3 Hz), 7.20 (m, 4H); 13 C NMR ($CDCl_3$, 75 MHz) δ 21.2, 21.5, 28.4, 28.8 (CH_2), 31.4 (CH_3), 26.9, 28.6, 38.2, 42.8, 53.0, 64.4, 123.4, 125.9, 126.0, 127.2 (CH), 138.1, 139.4 (C), 174.5 (CO); ν_{max} (CH2Cl$_2$) 3030w, 2940s, 2910s, 2865m, 1665s, 1485m, 1460m, 1400m, 1230m, 1180w, 1050w; MS *m/z* 267 (M+), 159*, 32, 28; HRMS calcd For $C_{18}H_{21}NO$ 267.1623; found: 267.1623.

4.1.4. Reduction of 10a with lithium aluminium hydride. The lactam **10a** (0.315 g; 1.18 mmol) was dissolved in dry diethyl ether (40 ml) and added to a slurry of lithium aluminium hydride (0.09 g; 2.37 mmol) in a small amount of diethyl ether. After reflux for 6 h, the excess hydride was destroyed by careful addition of diethyl ether which had been saturated with water. The mixture was filtered, dried, and the solvent evaporated under reduced pressure to give (**9**) as colourless crystals which were recrystallised from propanone/diethyl ether (80:20) to give a sample (0.24 g, 80%) mp 126–128°C; ^1H NMR data ($CDCl_3$) are summarised in Table 1; ^{13}C NMR ($CDCl_3$, 75 MHz) δ 26.3, 26.4 (CH_2), 44.5 (CH_3), 34.1, 39.7, 40.8, 46.4, 51.8, 62.0, 122.5, 124.2, 124.3, 125.0, 126.2, 131.7 (CH), 140.8, 143.7 (C); ν_{max} (CH_2Cl_2) 3005w, 2940s, 2860m, 2780w, 1480m, 1460m, 1175w, 1140w, 1110w, 830w; MS *m/z* 251 (M^+), 144*, 128, 114, 103, 78; HRMS calcd for $C_{18}H_{23}N$ 251.1674; found: 251.1674.

4.1.5. Reduction of 11a with lithium aluminium hydride. The lactam **11a** (0.195 g; 0.735 mmol) was dissolved in dry diethyl ether (30 ml), added to a slurry of lithium aluminium hydride (0.05 g; 1.47 mmol) in a small amount of ether, and treated as described for **9** to give **16** as colourless crystals (0.156 g, 85%), mp 83–85°C after recrystallisation from propanone/diethyl ether (80:20); ^1H NMR data ($CDCl_3$) are summarised in Table 1; ^{13}C NMR (CDCl^3, 75 MHz) δ 26.3, 26.6 (CH_2), 43.9 (CH_3), 33.1, 34.4, 40.2, 42.0, 45.8, 57.7, 62.5, 123.8, 125.1, 125.6, 126.9, 128.6, 128.8 (CH), 137.6, 140.4 (C); ν_{max} (CH_2Cl_2) 3005w, 2920s, 2850m, 2760w, 1460m, 1160w, 1130w, 1110w; MS *m/z* 251 (M^+), 144*, 128, 114, 103, 78; HRMS calcd for $C_{18}H_{23}N$ 251.1674; found: 251.1674.

4.1.6. Hydrogenation of 9 and 16. The amine **16** (30 mg) was dissolved in ethanol (ca. 5 ml) and hydrogenated over 5% palladium on carbon at atmospheric pressure for 6 h. The catalyst was filtered off through celite and the solvent

removed under reduced pressure to give an oily product (27 mg) which was dissolved in diethyl ether and shaken with dilute aqueous HCl (2×10 ml). The acid extracts were washed further with diethyl ether and the amine product regenerated by treatment with dilute aqueous NaOH, extraction into diethyl ether, and drying over $MgSO_4$. The product **18** was isolated as a crystalline solid but was not further purified: ^{1}H NMR data ($CDCl_3$, 400 MHz) δ 0.4 (m, 1H), 0.65–0.90 (m, 3H), 1.45–1.60 (m, 6H), 1.73 (dd, J=9.7, 2.4 Hz, 1H), 2.01 (s, 3H), 2.10 (br d, J=12 Hz, 1H), 2.47 (br d, J=12 Hz, 1H), 2.92 (pseudo-q, $J\approx$2.5 Hz, 1H), 3.36 (dd, J=9.7, 2.4 Hz, 1H), 3.52 (d, J=2.9 Hz, 1H), 7.1–7.3 (m, 4H); ^{13}C NMR ($CDCl_3$, 100 MHz) δ 21.7, 22.0, 28.8, 29.0, 58.9 (CH_2), 43.7 (CH_3), 27.2, 28.5, 40.0, 40.2, 44.1, 65.9, 124.8, 125.5, 125.8, 126.8 (CH), 137.9, 140.9 (C); ν_{max} (CH_2Cl_2) 3005w, 2940s, 2870m, 2770w, 1480m, 1460m, 1400m, 1185w, 1140w, 1110w, 810w; M.S. (ES) m/z 254 (MH^+); HRMS calcd for $C_{18}H_{24}N$ 254.1909; found: 254.1908.

Corresponding treatment of a small sample of **9** (ca. 5 mg) gave an oily sample which was shown to be different from **18** on the basis of a non-superimposable ^{1}H NMR spectrum which was too complex for full analysis. The compound was only tentatively identified as **17** and was not purified further on this small scale. A similar mass spectrum to that of **18** (MS (ES) m/z 254 (MH^+)) confirmed the molecular composition.

4.1.7. Reaction of 2-methyl-5,6-benzo-2-azabicyclo-[2.2.2]oct-7-ene-3-one 7 with cyclopenta-1,3-diene. To lactam **7** (2.0 g; 10.8 mmol) was added neat, freshly distilled cyclopenta-1,3-diene (3.56 g; 254.0 mmol)) in a Young's tube which was heated overnight (16 h) at 180°C. After cooling, the reaction mixture was placed on a silica column and the excess cyclopentadiene was washed off with petrol (bp 40–60°C). The column was then washed with diethyl ether to elute the reaction products (75%). TLC analysis showed only one spot but the ^{1}H NMR spectrum showed the presence of two cycloadducts **19** and **20** in a ratio of 65:35 but the compounds could not be separated chromatographically. Fractional crystallisation using propanone/diethyl ether (80:20) provided samples of both isomers. The adduct **19** (0.9 g; 33%) was isolated as colourless crystals, mp 123–125°C; ^{1}H NMR data ($CDCl_3$) are summarised in Table 1; ^{13}C NMR ($CDCl_3$, 75 MHz) δ 31.9 (CH_3), 44.6, 44.9, 45.0, 46.6, 51.1 (CH), 53.9 (CH_2), 62.0, 121.2, 124.0, 125.8, 126.9, 131.2, 132.4 (CH), 140.6, 142.5 (C), 172.1 (CO); ν_{max} (CH_2Cl_2) 2960m, 1668s; MS m/z 251 (M^+), 128*, 28; Analysis calcd for $C_{17}H_{17}NOC$ 81.45, H 6.74, N 5.51; found: C 81.24, H 7.00, N 5.66%.

The isomer **20** (0.45 g; 16%) was isolated as colourless crystals which contained traces of the isomer **19**; ^{1}H NMR data ($CDCl_3$) are summarised in Table 1; ^{13}C NMR ($CDCl_3$, 75 MHz) δ 31.6 (CH3), 41.5, 44.2, 45.6, 47.4, 51.3 (CH), 53.9 (CH_2), 62.9, 122.5, 125.1, 126.5, 127.8, 129.7, 130.1 (CH), 136.9, 138.6 (C), 175.2 (CO); ν_{max} (CH_2Cl_2) 2970m, 1668s; MS m/z 251 (M^+), 128, 28*; HRMS calcd for $C_{17}H_{17}NO$ 251.1310; found: 251.1310.

4.1.8. X-Ray structure analysis of 11a. Crystals of **11a** were obtained from propanone/diethyl ether (4:1). Crystal data. $C_{18}H_{19}NO$, M=265.34, orthorhombic, a=6.4990(13), b=13.533(5), c=15.910(6) Å, V=1399.3(5) Å^3 (by least squares refinement on diffractometer angles[16] for 447 centred reflections with 4.5<θ<14.5°, λ=0.71073 Å, T=293(2) K), space group $P2_12_12_1$, Z=4, Dc=1.260 mg m^{-3}, μ=0.077 mm^{-1}, F(000)=568. A tabular colourless crystal (0.27×0.26×0.11 mm^3) was used for the analysis.

Data collection and processing. A Stoe STADI-2 Weissenberg diffractometer with graphite monochromated Mo Kα radiation was used for data collection. The intensity data were collected using ω-scans, with scan range calculated from general inclination geometry and including Kα_1–Kα_2 separation, 1011 reflections were measured (3.95<θ<22.53°, 0≤h≤6, 0≤k≤14, 0≤l≤16) and corrected for Lorentz and polarisation effects, but not absorption. A standard reflection from each Weissenberg layer (constant h) was monitored every 50 reflections, no intensity decay was detected.

Structure solution and refinement. The structure was solved by direct methods and difference Fourier synthesis. Non-H atoms were refined anisotropically by full-matrix least squares techniques (on F^2, including all measured reflections with SHELXTL/PC[17]), H-atoms were in calculated positions and restrained to ride on their parent atoms with isotropic displacement parameters set to 1.3 times U_{eq} of their parent atoms. Data/restraints/parameters 1011/0/183, goodness of fit on F^2 1.065, final Rindices (all data), R_1=0.0702, wR_2=0.1311, [I>2(I)] R_1=0.0497, wR_2=0.1161. Maximum and minimum residual peak in the final difference Fourier map 0.150 and −0.201 e Å^{-3}. The molecular structure is shown in Fig. 1.

4.1.9. X-Ray structure analysis of 9. Crystals of **9** were obtained from propanone/diethyl ether (4:1). *Crystal data*. $C_{18}H_{21}N$, M=251.36, triclinic, a=6.298(2), b=10.694(2), c=11.021(2) Å, α=71.04(5), β=89.88(8), γ=77.22°, V=682.7(2) Å^3 (by least squares refinement on diffractometer angles[16] for 98 centred reflections with 3.9<θ<12.8°, λ=0.71073 Å, T=293(2) K), space group P-1, Z=2, Dc=1.223 mg m^{-3}, μ=0.070 mm^{-1}, F(000)=272. A tabular colourless crystal (0.24×0.23×0.046 mm^3) was used for the analysis.

Data collection and processing. A Stoe STADI-2 Weissenberg diffractometer with graphite monochromated Mo Kα radiation was used for data collection. The intensity data were collected using ω-scans, with scan range calculated from general inclination geometry and including Kα_1–Kα_2 separation, 1720 reflections were measured (3.78<θ<26.12°, −6≤h≤0, −11≤k10, −11≤l≤11) and corrected for Lorentz and polarisation effects, but not absorption. A standard reflection from each Weissenberg layer (constant h) was monitored every 50 reflections, no intensity decay was detected.

Structure solution and refinement. The structure was solved by direct methods and difference Fourier synthesis. Non-H atoms were refined anisotropically by full-matrix least squares techniques (on F^2, including all measured reflections with SHELXTL/PC[17]), H-atoms were in calculated

positions and restrained to ride on their parent atoms with isotropic displacement parameters set to 1.3 times U_{eq} of their parent atoms. Data/restraints/parameters 1708/0/173, goodness of fit on F^2 1.058, final R indices (all data), R_1=0.1058, wR_2=0.1324, [$I>2(I)$] R_1=0.0567, wR_2= 0.1089. Maximum and minimum residual peak in the final difference Fourier map 0.142 and -0.147 e Å^{-3}.The molecular structure is shown in Fig. 2. Crystallographic data (excluding structure factors) for the structures in this paper have been deposited with the Cambridge Crystallographic Data Centre as supplementary publication numbers CCDC 169448 (**9**) and CCDC 169447 (**11a**). Copies of the data can be obtained free of charge on application to CCDC, 12 Union Road, Cambridge CB2 1EZ, UK (fax: +44(0)-1223-336033, or e-mail: deposit@ccdc.cam.ac.uk).

Acknowledgements

We are grateful to the Algerian Government for financial support to D. B. We thank Dr Gerald Griffith for 15 N NMR spectra, Michael Lee for technical assistance, and Peter Holliman for some early development work.

References

1. Warrener, R. N. *Eur. J. Chem.* **2000**, 3363–3380 and references cited therein.
2. Rondan, N. G.; Paddon-Row, M. N.; Caramella, P.; Mareda, P.; Mueller, P.; Houk, K. N. *J. Am. Chem. Soc.* **1982**, *104*, 4974–4976. Spanget-Larsen, J.; Gleiter, R. *Tetrahedron* **1983**, *39*, 3345–3350.
3. Fieser, L. F.; Haddadin, M. J. *Can. J. Chem.* **1965**, *43*, 1599–1606.
4. Sasaki, T.; Manabe, T.; Nishida, S. *J. Org., Chem.* **1980**, *45*, 476–479.
5. Davies, J. W.; Durrant, M. L.; Walker, M. P.; Malpass, J. R. *Tetrahedron* **1992**, *48*, 4379–4398.
6. Belkacemi, D.; Davies, J. W.; Malpass, J. R.; Naylor, A.; Smith, C. R. *Tetrahedron* **1992**, *48*, 10161–10176.
7. Paquette, L. A.; Dunkin, I. R. *J. Am. Chem. Soc.* **1975**, *97*, 2243–2249 see also references in this paper to earlier work on related systems.
8. Williams, R. V.; Edwards, D.; Gadgil, V. R.; Colvin, M. E.; Seidl, E. T.; van der Helm, D.; Hossain, M. B. *J. Org. Chem.* **1998**, *63*, 5268–5271 and references therein.
9. Clearly, the 2-carbon N-containing bridge in (**10**) and (**11**) should take priority in defining the terms *exo-* and *endo-* with respect to the facial attack on (**7**) but this unfortunately reverses the terminology with respect to the norbornyl and hetero-norbornyl adducts in Scheme 1. In this paper, we prefer to use the benzo-group as the point of reference to allow direct comparisons between both systems with a minimum of confusion.
10. Margetic, D.; Warrener, R. N.; Malpass, J. R. *Internet J. Chem.* **1999**, *2,* article 6, http://www.ijc.com/articles/1999v2/6/.
11. Davies, J. W.; Durrant, M. L.; Walker, M. P.; Belkacemi, D.; Malpass, J. R. *Tetrahedron* **1992**, *48*, 861–884.
12. Belkacemi, D.; Malpass, J. R. *Tetrahedron* **1993**, *49*, 9105–9116.
13. Malpass, J. R.; Butler, D. N.; Johnston, M. R.; Hammond, M. L. A.; Warrener, R. N. *Org. Lett.* **2000**, *2*, 721–724 and references cited therein.
14. Work with hetero-bridged polynorbornane systems shows that flattening at nitrogen is associated with upfield shifts in ^{15}N NMR specta: Malpass, J. R.; Warrener, R. N.; Butler, D. N.; Johnston, M. R. Manuscript in preparation.
15. Sheinin, E.; Wright, G.; Bell, C. *J. Heterocycl. Chem.* **1968**, *5*, 859–862 for fuller spectroscopic data, see Ref. 12.
16. Clegg, W.; Sheldrick, G. M. *Z. Kristallogr.* **1984**, *167*, 23–27.
17. Sheldrick, G. M. *SHELXTL/PC*; Siemens Analytical X-ray Instruments: Madison, WI, 1996.